Cancer Chemotherapy and Pharmacology (2018) 81:1095–1103
https://doi.org/10.1007/s00280-018-3572-1

ORIGINAL ARTICLE

Cabazitaxel is more active than first-generation taxanes in *ABCB1*(+) cell lines due to its reduced affinity for P-glycoprotein

George E. Duran[1] · Volker Derdau[2] · Dietmar Weitz[2] · Nicolas Philippe[3] · Jörg Blankenstein[3] · Jens Atzrodt[2] · Dorothée Sémiond[4] · Diego A. Gianolio[4] · Sandrine Macé[3] · Branimir I. Sikic[1]

Received: 16 February 2018 / Accepted: 26 March 2018 / Published online: 19 April 2018

Abstract

Purpose The primary aim of this study was to determine cabazitaxel's affinity for the *ABCB1*/P-glycoprotein (P-gp) transporter compared to first-generation taxanes.

Methods We determined the kinetics of drug accumulation and retention using [^{14}C]-labeled taxanes in multidrug-resistant (MDR) cells. In addition, membrane-enriched fractions isolated from doxorubicin-selected MES-SA/Dx5 cells were used to determine sodium orthovanadate-sensitive ATPase stimulation after exposure to taxanes. Custom [^{3}H]-azido-taxane analogues were synthesized for the photoaffinity labeling of P-gp.

Results The maximum intracellular drug concentration was achieved faster with [^{14}C]-cabazitaxel (5 min) than [^{14}C]-docetaxel (15–30 min). MDR cells accumulated twice as much cabazitaxel than docetaxel, and these levels could be restored to parental levels in the presence of the P-gp inhibitor PSC-833 (valspodar). Efflux in drug-free medium confirmed that MDR cells retained twice as much cabazitaxel than docetaxel. There was a strong association ($r^2 = 0.91$) between the degree of taxane resistance conferred by P-gp expression and the accumulation differences observed with the two taxanes. One cell model expressing low levels of P-gp was not cross-resistant to cabazitaxel while demonstrating modest resistance to docetaxel. Furthermore, there was a 1.9× reduction in sodium orthovanadate-sensitive ATPase stimulation resulting from treatment with cabazitaxel compared to docetaxel. We calculated a dissociation constant (Kd) value of 1.7 µM for [^{3}H]-azido-docetaxel and ~7.5 µM for [^{3}H]-azido-cabazitaxel resulting in a 4.4× difference in P-gp labeling, and cold docetaxel was a more effective competitor than cabazitaxel.

Conclusion Our studies confirm that cabazitaxel is more active in *ABCB1*(+) cell models due to its reduced affinity for P-gp compared to docetaxel.

Keywords *ABCB1* · P-glycoprotein · Cabazitaxel · Multidrug resistance · Taxanes

Introduction

Intrinsic or acquired drug resistance limits the clinical efficacy of the microtubule-stabilizing agents, paclitaxel and docetaxel. Resistance mechanisms include alterations in drug targets such as mutations in β-tubulin [1], epithelial to mesenchymal transition [2–5], the expression of cell cycle regulators [5–11], and defects in apoptotic pathways [12–14]. However, a major mechanism of resistance resulting from long-term drug selection with taxanes in cell lines is the activation of *ABCB1*/P-gp [15–18], a 170-kDa transmembrane ATP-binding cassette (ABC) transporter which confers high levels of resistance to a wide range of structurally unrelated substrates. This resistance can be

Electronic supplementary material The online version of this article (https://doi.org/10.1007/s00280-018-3572-1) contains supplementary material, which is available to authorized users.

✉ George E. Duran
george.duran@stanford.edu

1 Division of Oncology, Department of Medicine, Stanford University School of Medicine, CCSR North 1120, 269 Campus Drive, Stanford, CA 94305-5151, USA

2 Sanofi R&D, Frankfurt, Germany

3 Sanofi R&D, Vitry-sur-Seine, France

4 Sanofi Oncology, Cambridge, MA, USA

modulated in the presence of known MDR reversal agents that inhibit transport.

Cabazitaxel (Jevtana®), the dimethoxy derivative of docetaxel, was developed based on its superior activity compared to first-generation taxanes in a number of taxane-resistant tumor models, including the melanoma model B16/TXT with acquired resistance to docetaxel [19], as well as its ability to bypass efflux transporters expressed in the blood–brain barrier [20]. This current study assessed cabazitaxel activity in MDR models and we confirmed that it is more active than paclitaxel and docetaxel. We investigated cabazitaxel's affinity for P-gp using accumulation and retention studies, ATPase stimulation, and direct photolabeling of P-gp using novel azido-taxanes to further understand its improved activity in *ABCB1*(+) models of taxane resistance.

Materials and methods

Drugs and reagents

Docetaxel (XRP6976, Taxotere®) and cabazitaxel (XRP6258, Jevtana®) were kindly provided by Sanofi Oncology (Vitry-sur-Seine, France). Novartis Pharmaceuticals (East Hanover, NJ) supplied the P-gp inhibitor PSC-833 (valspodar). Other chemotherapeutic drugs used in this study were obtained from the drug repository of the U.S. National Cancer Institute (Bethesda, MD). Drugs were prepared in 100% ethanol as 1 mmol/L stock solutions and stored at − 20 °C.

Chemical synthesis of radio- and azido-taxanes

The [propionyl-3-^{14}C]-taxanes (docetaxel: 2.58 MBq/mg; cabazitaxel: 2.50 MBq/mg, Supplementary Figure S1) used for drug accumulation and retention studies were provided by the Isotope Chemistry and Metabolite Synthesis (ICMS) department of Sanofi (Frankfurt, Germany). The same group synthesized novel azido-taxane analogues used in the photoaffinity labeling of P-gp. Briefly, the azido function was incorporated via a common oxazolidine intermediate by regioselective iodination of the aromatic para-position applying iodine and phenyliodine bis(trifluoroacetate) (PIFA), and a subsequent copper-catalyzed, electrophilic substitution with sodium azide (Web Supplement: Chemical synthesis of tritium and azido-labeled taxanes). Final [phenyl-3,5-$^{3}H_2$]-azido taxanes (Supplementary Figure S2) had a specific activity of 2.08 and 2.15 GBq/mg for docetaxel and cabazitaxel, respectively.

Cell culture and establishment of MDR variants

The MCF-7 human breast adenocarcinoma and the OVCAR-3 human ovarian adenocarcinoma cell lines were purchased from the American Type Culture Collection (ATCC, Manassas, VA, purchased 6/1999). In addition, several MCF-7 variants were used in this study including MCF-7/TxT50 and MCF-7/CTAX selected by us with docetaxel or cabazitaxel alone. These variants are positive for P-gp/*ABCB1* and demonstrate a typical MDR phenotype [5]. *ABCB1*/P-gp is expressed at high levels in the long-term, stepwise doxorubicin-selected human uterine sarcoma MDR variant MES-SA/Dx5 cells (authenticated and submitted to the ATCC as CRL-1977, Supplemental Figure S3A, 21), and is the predominant mechanism of resistance in these cells, with minimal expression of other ABC transporters as determined by microarray analysis (Supplemental Figure S3B). The variant cell line MES-SA/Dx0.5 expresses low levels of drug resistance and low levels of P-gp. MES-SA cells were continuously exposed to paclitaxel alone in a step-wise manner to a final concentration of 30 nmol/L to establish the *ABCB1*(+) MDR model, MES-SA/T30 [21]. Finally, the daunorubicin-selected human erythroleukemic MDR variant, K562/R7 (Cellosaurus: Accession CVCL-D573), also expresses high levels of P-gp as its major mechanism of resistance [22–24]. All MDR variants were exposed to the selecting agent for at least three passages, followed by two drug-free passages prior to use.

Cells were grown in McCoy 5A medium supplemented with 10% (v/v) fetal bovine serum, 100 U of penicillin/mL, and 100 µg of streptomycin/mL (all Corning Mediatech, Manassas, VA) at 37 °C in a humidified atmosphere containing 5% CO_2. Cells were routinely screened to rule out mycoplasma infection.

Growth inhibition assays

The in vitro activity of various anticancer drugs was tested using a modified sulforhodamine B (SRB) assay [25] for adherent cells, or 3-(4,5-dimethylthiazol-2-yl)-2,5-diphenyltetrazolium bromide (MTT) assay [17] for suspension cells following a 72-h drug incubation representing approximately three cell divisions. Drug effects were calculated as a percentage relative to untreated control survival, and response versus drug concentration was calculated using the Hill equation in KaleidaGraph software (Synergy Software, Reading, PA). Each drug concentration was tested in quadruplicate measurements per experiment, and data presented are the average of three independent experiments ± standard deviations.

Western blotting

The expression of proteins was determined by Western blotting using the following antibodies: anti-P-gp (clone C219, Signet Laboratories, Dedham, MA), anti-α-tubulin (clone DM1A, Sigma-Aldrich, St. Louis, MO), and anti-GAPDH (clone D16H11, Cell Signaling Technology, Danvers, MA). These primary antibodies were recognized by species-appropriate horseradish peroxidase-conjugated secondary antibodies, and detected using the Clarity Western ECL substrate on a ChemiDoc MP Imaging System (Bio-Rad, Hercules, CA).

Microarray analysis of ABC transporters

mRNA from MES-SA/Dx5 cells was isolated using the FastTrack kit (Invitrogen Life Technologies, Carlsbad, CA) and hybridized to GeneChip Human Genome U133 Plus 2.0 Array (Affymetrix, Santa Clara, CA).

Tubulin polymerization assay

Soluble and polymerized tubulin fractions were separated by centrifugation (20,000×*g*) following a 5 min incubation in hypotonic buffer with and without drug at 37 °C [1, 5, 26]. The soluble tubulin fractions were transferred to fresh microcentrifuge tubes and stored on ice, while fractions containing polymerized tubulin were sonicated for 10 s on ice prior to adding 4× Laemmli sample buffer (Bio-Rad). Equal volumes of soluble and polymerized fractions were resolved on gradient polyacrylamide gels, transferred to nitrocellulose, and probed with a pan α-tubulin antibody.

Functional assays for transporter activity

Taxane accumulation patterns were studied using [^{14}C]-radiolabeled docetaxel and cabazitaxel over a time course up to 1 h. Time points were collected and spun (10,000×*g*, 1 min) through Nyosil M20 oil (New Bedford, MA) thereby terminating uptake, cell pellets were lysed with 2% (w/v) SDS. Counts were determined using EcoLite scintillation cocktail (MP Biomedicals, Solon, OH), and normalized to protein content. Efflux in drug-free medium followed collecting time points for up to 1 h.

Drug-stimulated ATPase activity

ATPase stimulation was measured as a function of the release of inorganic phosphates from ATP hydrolysis following drug treatment using the Corning Gentest ATPase assay (BD Biosciences, Woburn, MA). Membranes were isolated from MES-SA/Dx5 cells using a published protocol [27], and results confirmed using membranes isolated from insect cells infected with human *ABCB1* cDNA using a baculovirus expression system (BD Biosciences) compared to membranes isolated from insect cells infected with wild-type virus. Membranes were incubated with drug for 5 min at 37 °C in the presence and absence of ATP, followed by additional 30 min incubation prior to the addition of a colorimetric reagent according to the manufacturer's protocol. All conditions were run with and without sodium orthovanadate, and microtiter plates were read at 800 nm on a SpectraMax Paradigm (Molecular Devices, Sunnyvale, CA).

Photoaffinity labeling of P-gp

Isolated membranes of MES-SA/Dx5 cells were incubated with [^{3}H]-azido-taxanes at 25 °C for 1 h, and irradiated on ice for 30 min with a UV lamp (366 nm) at a distance of 8 cm. Photolabeled membranes were analyzed by SDS-polyacrylamide gel electrophoresis, fixed in isopropanol:water:acetic acid solution (25:65:10) for 30 min, soaked in Amplify Fluorographic Reagent (GE Healthcare Life Sciences, Pittsburgh, PA), and dried prior to exposing to film.

Results

Cabazitaxel is more active than first-generation taxanes in P-gp(+) cell models

Taxane sensitivity was tested in MDR models that express low (MES-SA/Dx0.5), moderate (MCF-7/CTAX), and high levels of P-gp (MES-SA/Dx5, MES-SA/T30, K562/R7, and MCF-7/TxT50), and the cell models with the highest expression of P-gp were the most resistant to docetaxel and paclitaxel (Table 1). Although the taxane-resistant variants were cross-resistant to cabazitaxel, the drug was 1.8–17-fold more active than first-generation compounds under identical experimental conditions. Sensitivity was restored to parental levels by including the P-gp inhibitor PSC-833 (2 μmol/L).

P-gp cell models accumulate and retain more cabazitaxel than docetaxel

[^{14}C]-labeled taxanes with equivalent-specific activities were synthesized and used to determine the drug accumulation patterns in MES-SA/Dx5 compared to parental MES-SA cells over a time course up to 1 h. We observed a difference in the kinetics of the accumulation between the two taxanes, with the maximum intracellular drug concentration achieved much faster with cabazitaxel (5 min) than docetaxel (15–30 min, Fig. 1a). MES-SA/Dx5 cells accumulated less taxane compared to parental cells, and these levels could be restored in the presence of 2 μmol/L PSC-833. Although the steady-state concentrations for both taxanes were equivalent

Table 1 Cabazitaxel activity compared to other P-gp substrates in three MDR models: the doxorubicin-selected MES-SA/Dx5, the paclitaxel-selected MES-SA/T30, and the daunorubicin-selected K562/R7

	Relative resistance[a] (modulation by PSC-833)[b]		
	MES-SA/Dx5	MES-SA/T30	K562/R7
Docetaxel	1200 ± 95 (1.5 ± 0.52)	60 ± 5.6 (1.0 ± 0.13)	80 ± 7.3 (1.9 ± 0.38)
Paclitaxel	1400 ± 70 (1.0 ± 0.16)	56 ± 6.2 (1.2 ± 0.11)	78 ± 2.6 (3.0 ± 0.34)
Cabazitaxel	210 ± 13 (1.3 ± 0.13)	11 ± 1.8 (1.1 ± 0.22)	4.7 ± 0.45 (0.93 ± 0.09)
Vinblastine	1500 ± 85 (1.5 ± 0.18)	66 ± 9.8 (1.0 ± 0.15)	95 ± 8.5 (2.3 ± 0.44)
Vincristine	1500 ± 160 (1.3 ± 0.25)	59 ± 8.3 (1.2 ± 0.13)	97 ± 9.3 (1.5 ± 0.19)
Colchicine	1700 ± 250 (1.8 ± 0.35)	40 ± 6.5 (1.0 ± 0.17)	94 ± 8.2 (1.2 ± 0.18)
Daunorubicin	75 ± 9.8 (1.5 ± 0.19)	13 ± 1.8 (1.2 ± 0.10)	12 ± 2.7 (1.9 ± 0.91)
Doxorubicin	70 ± 5.9 (1.8 ± 0.33)	15 ± 2.2 (1.5 ± 0.24)	10 ± 1.8 (1.5 ± 0.28)
Cisplatin	2.2 ± 0.51 (1.5 ± 0.30)	1.3 ± 0.16 (1.2 ± 0.21)	1.1 ± 0.05 (1.7 ± 0.27)

SRB or MTT assays were run following 72-h drug incubations with and without PSC-833 (2 µmol/L). Data are expressed as the mean of three independent determinations ± standard deviations. Sensitivity data in the remaining MDR models included in this study were previously published [5]

[a]The relative resistance was calculated by dividing the IC_{50} value of the variant by the IC_{50} of the wild-type cell line

[b]Relative resistance following co-incubation with the P-gp inhibitor PSC-833 at 2 µmol/L

in parental MES-SA cells, MES-SA/Dx5 accumulated 2.1-fold more cabazitaxel than docetaxel (64–30% of MES-SA levels, $p = 0.0004$). Following the 1 h drug accumulation, taxane efflux was measured in drug-free medium at 37 °C for an additional hour. MES-SA/Dx5 cells retained 3.6-fold more cabazitaxel than docetaxel ($p < 0.0001$, Supplementary Figure S4).

These data were substantiated in other P-gp cell models including a less resistant variant of MES-SA (MES-SA/Dx0.5), several docetaxel- and paclitaxel-selected human ovarian cancer cell lines, and the human erythroleukemic MDR variant K562/R7. Cabazitaxel levels were 89% of parental K562 levels versus 50% in cells exposed to docetaxel (1.8-fold difference, $p < 0.0001$, Fig. 1b), and co-incubation with PSC-833 completely inhibited P-gp function and restored drug to parental levels.

The accumulation patterns of both docetaxel and cabazitaxel revealed a strong association with the degree of taxane resistance conferred by P-gp. These accumulation profiles correlated with the degree of resistance observed to each taxane in cytotoxicity assays ($n = 28$, $r^2 = 0.91$, Fig. 1c), confirming that P-gp transported and conferred more resistance to docetaxel than to cabazitaxel in each MDR cell model tested. Included in this analysis is the low *ABCB1*/P-gp(+) MES-SA/Dx0.5 cell model which was not resistant to cabazitaxel while demonstrating modest resistance to docetaxel and paclitaxel.

Reduced ATPase stimulation following treatment with cabazitaxel than docetaxel

As an indirect measure of P-gp activity, we determined the degree of ATPase stimulation resulting from exposure to each taxane over a dose range (1 nmol/L to 5 µmol/L) using membranes isolated from MES-SA/Dx5 (Fig. 2a). The peak vanadate-sensitive ATPase activity was achieved at 500 nmol/L for cabazitaxel and 1 µmol/L for docetaxel, with 1.9-fold more ATPase stimulation observed with docetaxel than with cabazitaxel at 1 µmol/L (37 vs. 18 nmol/mg/min, $p = 0.0002$). Km values were comparable for both docetaxel and cabazitaxel (65 nmol/L), but the Vmax value for docetaxel was twice that of cabazitaxel, resulting in a 2-fold higher efflux clearance ($CL_{Efflux} = Vmax/Km$) for docetaxel compared to cabazitaxel. The P-gp inhibitor verapamil was included as a positive control for ATPase stimulation, and a peak of 13 nmol/mg/min was obtained at 1 µM under the same experimental conditions.

Results were confirmed using membranes isolated from High Five (BTI-TN5B1-4) insect cells infected with human *ABCB1* cDNA using a baculovirus expression system (BD Biosciences, Fig. 2b). Vanadate-sensitive ATPase activity was measured following exposure to docetaxel or cabazitaxel (both at 1 µmol/L), and verapamil (5 µmol/L) was used as a positive control. We observed 1.5-fold higher ATPase activity in the conditions containing docetaxel compared to cabazitaxel ($p = 0.0058$). No vanadate-sensitive ATPase activity was observed following exposure to either taxanes or verapamil in membranes isolated from High Five cells infected with control baculovirus (data not shown).

Reduced photoaffinity labeling of P-gp with cabazitaxel than docetaxel

Taxanes modified with photoreactive azido moieties have been used to probe the paclitaxel binding site on microtubules and P-gp [28–31]. In this new synthesis

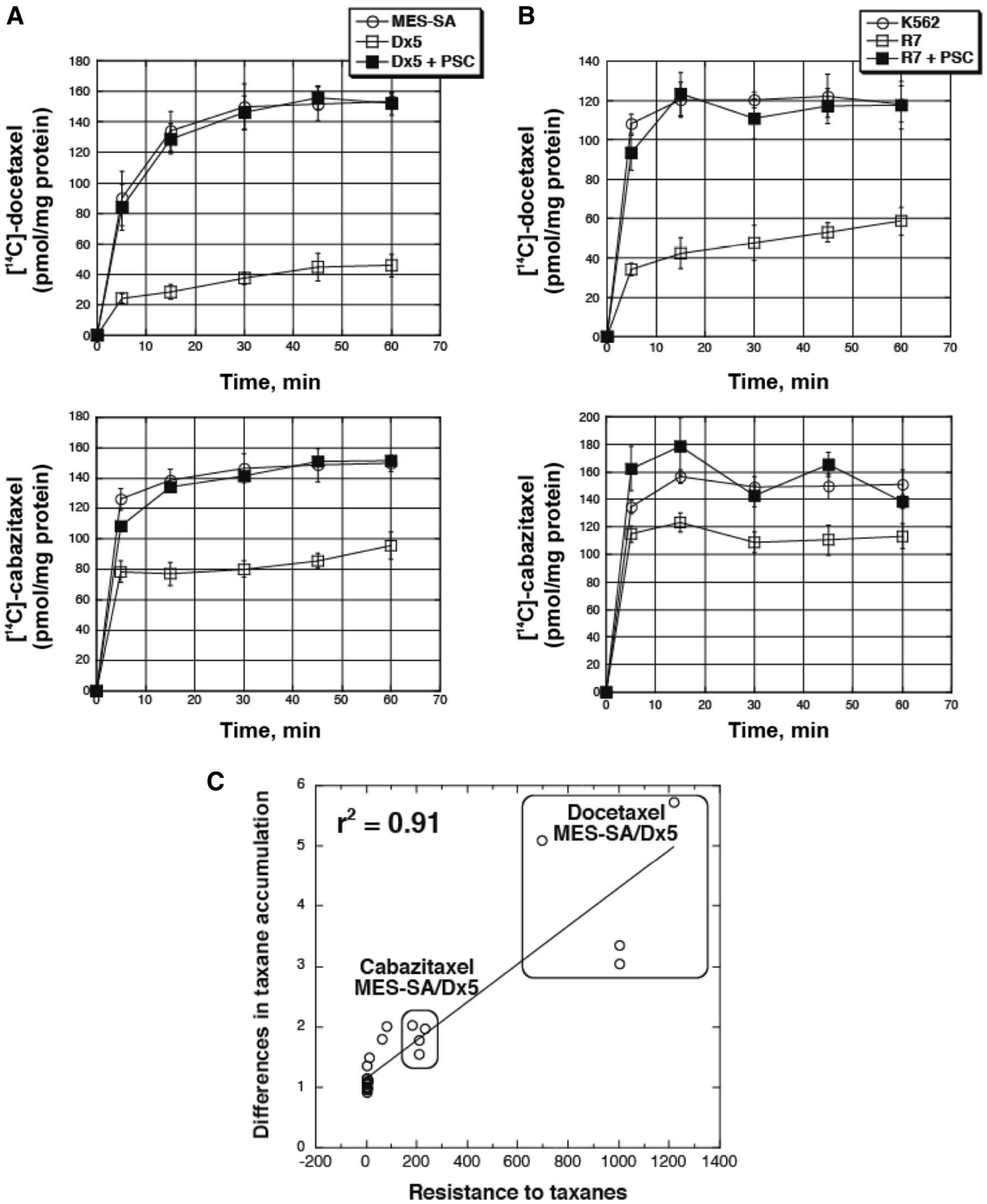

Fig. 1 The kinetics of taxane accumulation in MDR models was assessed using 1 µmol/L [^{14}C]-labeled docetaxel or cabazitaxel over a time course (5–60 min). Separate experimental conditions included the P-gp inhibitor PSC-833 (PSC, 2 µmol/L). Samples containing 1.5×10^6 MES-SA/Dx5 (**a**) or K562/R7 (**b**) cells were collected and centrifuged through Nyosil M20 oil (10,000×*g*, 1 min) to terminate drug accumulation at the appropriate time point. Medium and oil were aspirated, cell pellets lysed in a 2% (w/v) SDS solution, and counts determined by liquid scintillation. Measurements are expressed as the mean of triplicate samples normalized to protein content ± standard deviations. There was a strong correlation between the difference in taxane accumulation between the MDR models tested and their parental controls in our uptake assays and the degree of taxane resistance conferred by P-gp. A total of 28 samples were included in this analysis including conditions run with PSC-833 ($r^2 = 0.91$, **c**). Two populations are highlighted: results with docetaxel alone and cabazitaxel alone, both in MES-SA/Dx5 cells

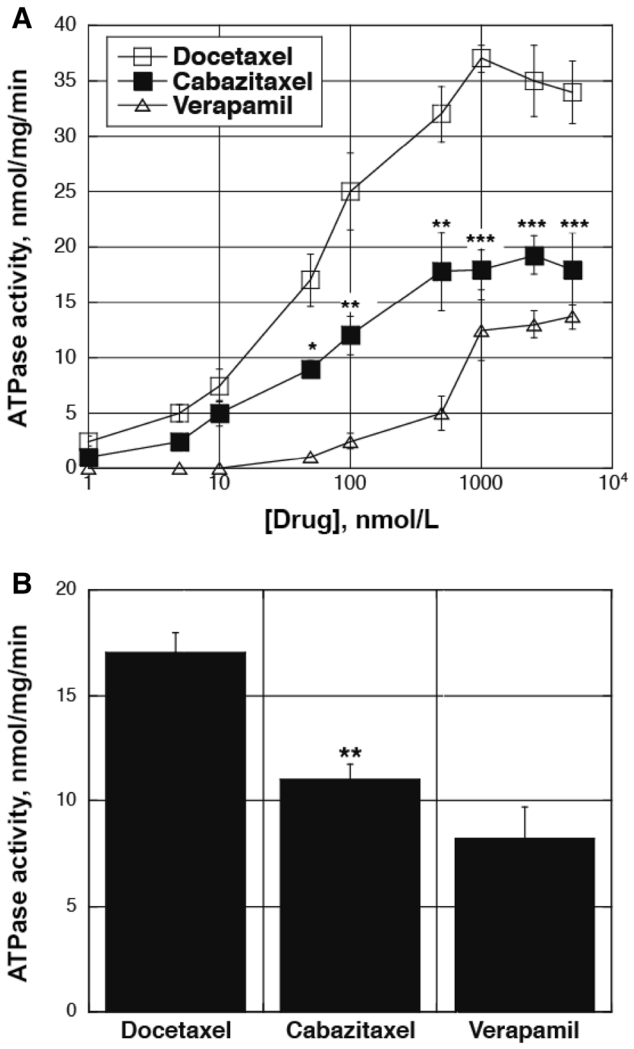

Fig. 2 An ATPase assay was used to determine P-gp activity following taxane treatment. Membranes isolated from the MDR model MES-SA/Dx5 (5 mg/mL) were preincubated with either docetaxel or cabazitaxel over a dose range (1 nmol/L to 5 µmol/L) for 5 min at 37 °C, followed by the addition of ATP and an additional 30 min incubation at 37 °C. A stop solution was added to each well along with a colorimetric reagent supplied by the manufacturer (Corning Gentest). The plate was read on a multiwell spectrophotometer at 800 nm. Conditions were run with and without sodium orthovanadate, and the P-gp inhibitor verapamil was included as a positive control for ATPase stimulation. All data are expressed as the average stimulated ATPase activity for each substrate ± standard deviation, with significance determined between the readings following docetaxel or cabazitaxel exposure per concentration tested (unpaired *t* test, $*p<0.05$, $**p<0.01$, $***p<0.001$, **a**). Results were confirmed using membranes isolated from High Five (BTI-TN5B1-4) insect cells infected with baculovirus containing human *ABCB1* cDNA. Vanadate-sensitive ATPase activity was measured following exposure to docetaxel or cabazitaxel (both at 1 µmol/L), and verapamil (5 µmol/L) was used as a positive control for ATPase activity. Data are presented as a mean of triplicate measurements ± standard deviation ($p=0.0058$, **b**)

of azido-docetaxel and cabazitaxel analogues, modifications of the taxane ring were excluded to avoid changes in P-gp binding affinity. This was confirmed by accumulation assays with these novel [^{3}H]-azido-taxanes in MES-SA/Dx5 that resulted in similar uptake profiles after 60 min as previously reported with the [^{14}C]-taxanes (Fig. 3a). [^{3}H]-azido-cabazitaxel levels were higher than [^{3}H]-azido-docetaxel in MES-SA/Dx5 (52 vs. 30% of MES-SA levels, $p=0.024$), and these levels were restored to parental levels in the presence of 2 µmol/L PSC-833.

The ability of these azido-taxanes to bind to tubulin polymer and to stabilize microtubules was also tested in a non-MDR cell line. Immunoblotting with a pan α-tubulin monoclonal antibody revealed increased tubulin polymer in OVCAR-3 cells exposed to 100 nmol/L [^{3}H]-azido-taxanes relative to untreated controls (Fig. 3b), and there was no significant difference in microtubule-stabilizing activity between the two azido-taxanes. Furthermore, a clear signal was observed in the tubulin polymer fraction following fluorography in [^{3}H]-azido-taxane-labeled proteins.

Membrane fractions (100 µg) isolated from MES-SA/Dx5 cells were exposed to [^{3}H]-azido-taxanes (100 nmol/L to 25 µmol/L) and UV irradiated for 30 min at 366 nm. A dose-dependent signal was detected following fluorography for each azido-taxane with a Bmax achieved at 5 µmol/L azido-docetaxel (Fig. 3c). A Bmax for azido-cabazitaxel was not achieved and higher concentrations of the drug could not be tested due to the ethanol content in the stock. We calculated a Kd value of 1.7 µmol/L for docetaxel and approximately 7.5 µmol/L for cabazitaxel, representing a 4.4-fold difference in binding to P-gp present in MES-SA/Dx5 (Fig. 3d).

Keeping the azido-taxane concentration constant at 25 µmol/L, we varied the membrane concentration from 0.78 to 100 µg. There was a 5-fold difference in P-gp labeling with more azido-docetaxel signal present than azido-cabazitaxel (Fig. 4a, b). Finally, in a separate experiment, we added cold docetaxel and cabazitaxel (1–25 µmol/L) to conditions which included [^{3}H]-azido-taxanes at 25 µmol/L. Cold taxanes competed with the azido-taxanes for P-gp labeling, but cold docetaxel was more competitive than cabazitaxel at the same concentrations (Fig. 4c). No signal was present in each of the cold docetaxel conditions, while a faint signal was present with cold cabazitaxel at 1 and 5 µmol/L.

Several other ABC transporters have been found to be associated with taxane resistance including *ABCC1*/MRP1, *ABCC2*/MRP2, and *ABCG2*/BCRP [32]. Following the same photoaffinity labeling protocol, we did not observe bands at the appropriate molecular weight using commercially available membrane preparations isolated from High Five insect cells expressing human *ABCC1, ABCC2* or *ABCG2* (data not shown).

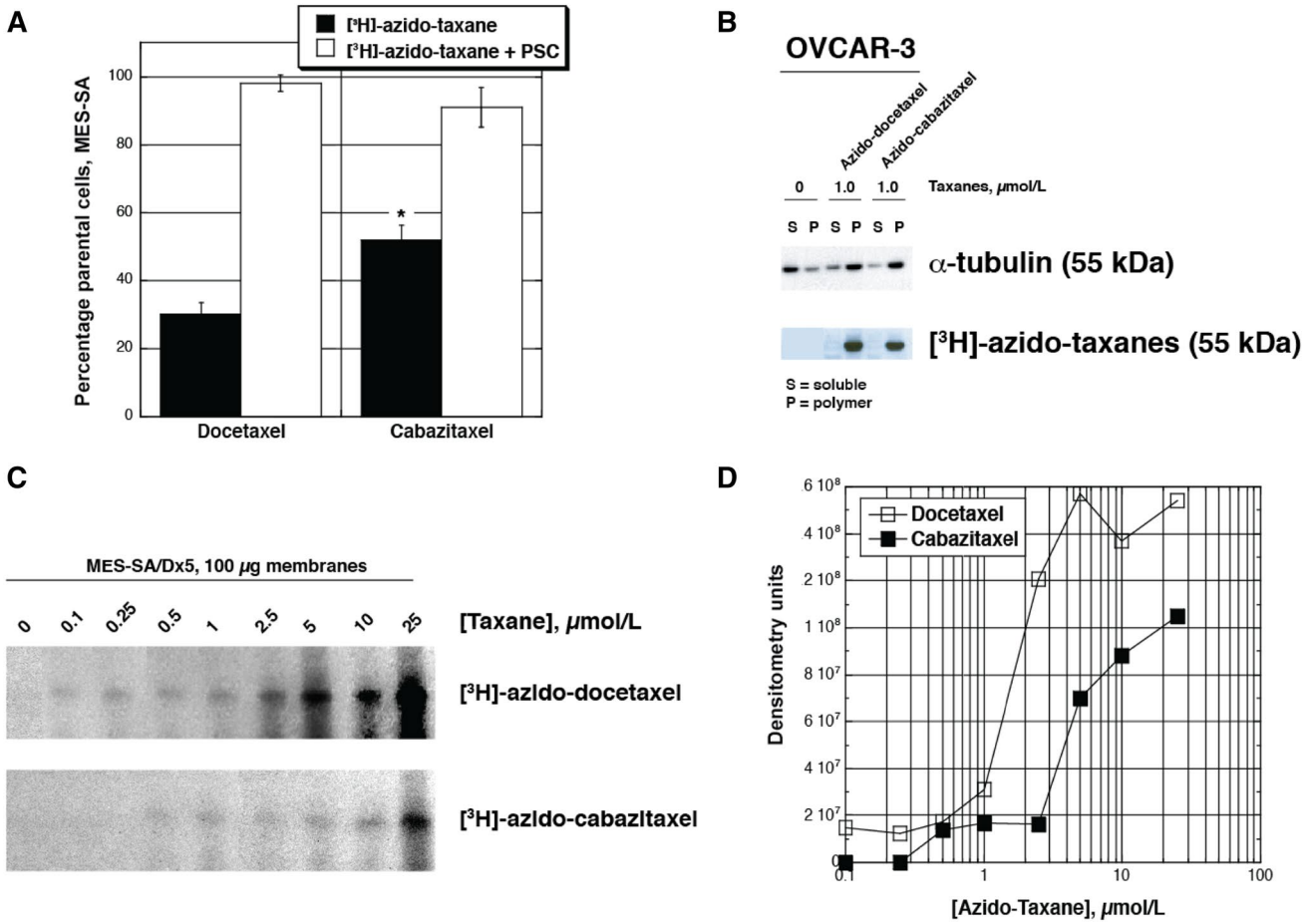

Fig. 3 Accumulation profiles of [^{3}H]-azido-taxane analogues were assessed in MES-SA/Dx5 cells following a 1 h exposure at 37 °C. Data are expressed as the percentage of parental MES-SA cells ± standard deviation ($n = 3$ per condition), with significance determined between [^{3}H]-azido-docetaxel and [^{3}H]-azido-cabazitaxel without PSC-833 (unpaired t test, $*p < 0.05$, **a**). Tubulin polymer was separated from soluble tubulin by centrifugation (20,000×g) following 5 min incubation in hypotonic buffer with and without drug (azido-taxanes, 1 μmol/L) at 37 °C in the dark, and fractions were resolved on 4–20% gradient polyacrylamide gels and transferred to nitrocellulose. Immunoblotting with a pan β-tubulin antibody (clone DM1A, Sigma-Aldrich) isolated the tubulin fractions in the human ovarian cancer cell line, OVCAR-3 (**b**). In a separate experiment, crude tubulin preparations were exposed to azido-taxanes (1 μmol/L) in the dark, UV-irradiated at 366 nm (30 min on ice), exposed to Amplify Fluorographic Reagent (GE Healthcare Life Sciences), gels dried, and exposed to film. Membrane-enriched fractions (100 μg) isolated from the MDR model MES-SA/Dx5 were labeled with [^{3}H]-azido-taxanes (100 nmol/L to 25 μmol/L) following 1 h exposure in the dark (**c**). Following UV irradiation at 366 nm (30 min on ice), samples were electrophoresed on 4–20% SDS-polyacrylamide gels and visualized by fluorography. Bands were quantitated on a Gel Doc XR+ imaging system (Bio-Rad, Hercules, CA) and dissociation constant (Kd) values were calculated from semi-logarithmic curves (**d**)

Discussion

Cabazitaxel was identified and subsequently selected for clinical development due to its activity in cancer models that were resistant to paclitaxel and docetaxel [19]. Our study confirms that cabazitaxel is more active than paclitaxel and docetaxel in cells that express the *ABCB1*/P-gp transporter. Although our cell models were cross-resistant to cabazitaxel, the resistance observed was lower than the resistance observed to either paclitaxel or docetaxel. The resistance to all taxanes was sensitive to modulation by P-gp inhibitors, resulting in complete sensitization to parental levels with 2 μmol/L PSC-833. Moreover, cells with low levels of P-gp were not cross-resistant to cabazitaxel while demonstrating resistance to other taxanes.

To better understand cabazitaxel's improved activity, we determined taxane accumulation and retention profiles in several MDR models and found that higher levels of cabazitaxel were achieved relative to docetaxel. The accumulation differences observed between the MDR variants and their respective parental controls were highly associated with the degree of taxane resistance observed in our colorimetric cell sensitivity assays, indicating that P-gp transport was responsible for the differences in activity between the two taxanes

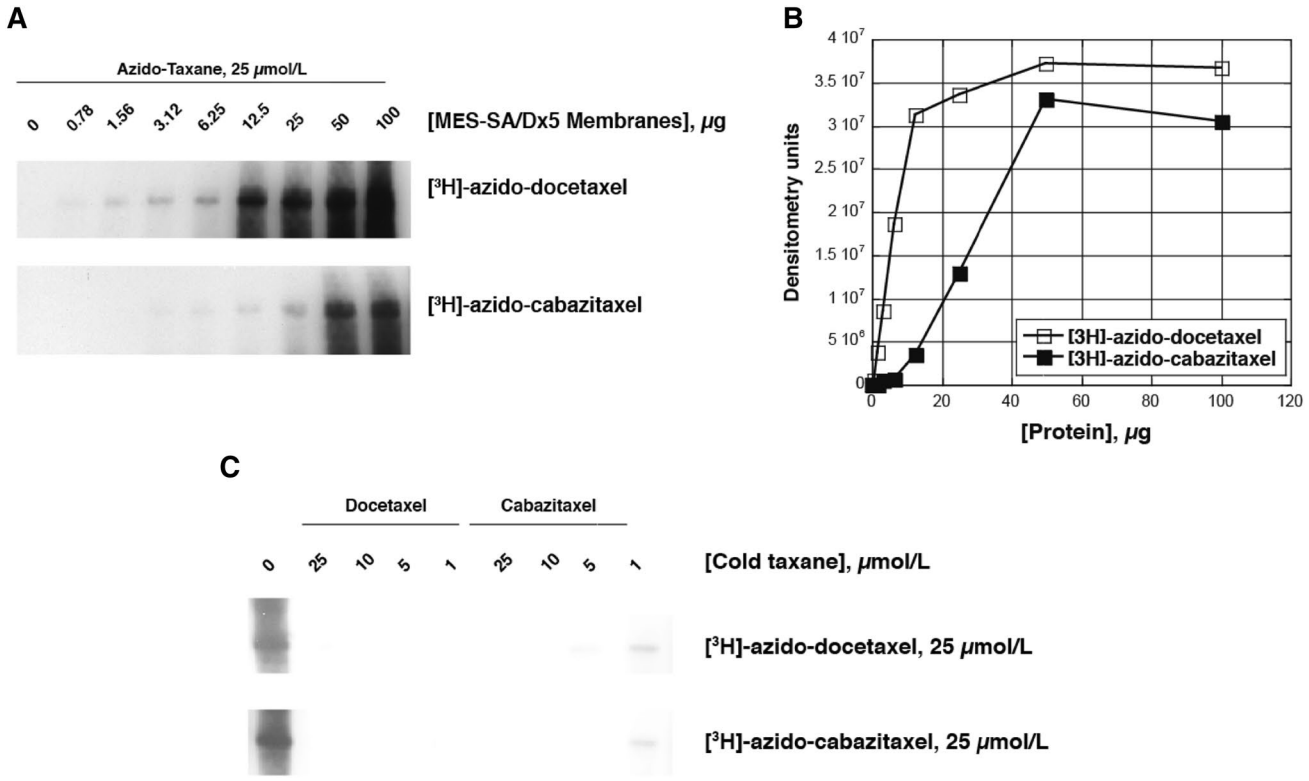

Fig. 4 A range of membrane fraction concentrations (0.78–100 μg) from the MDR model MES-SA/Dx5 were labeled with 25 μmol/L [^{3}H]-azido-taxanes and visualized by fluorography (**a**). Densitometry is presented in **b**. Membranes (100 μg) from MES-SA/Dx5 were exposed to cold taxanes (either docetaxel or cabazitaxel, 1–25 μmol/L) prior to labeling with 25 μmol/L [^{3}H]-azido-taxanes (**c**)

in our cell models. We also found that docetaxel stimulated twice as much vanadate-sensitive ATPase and had a 2-fold higher CL_{Efflux} compared to cabazitaxel in P-gp-enriched membranes isolated from MES-SA/Dx5 cells.

Direct photolabeling of P-gp with novel photoreactive radiolabeled azido-taxanes confirmed a 4.4-fold lower Kd for docetaxel than cabazitaxel using membranes isolated from MES-SA/Dx5 cells. Several other ABC transporters are associated with taxane resistance including *ABCC1*/MRP1, *ABCC2*/MRP2, and *ABCG2*/BCRP. However, no bands were observed at the appropriate molecular weight following photoaffinity labeling with azido-taxanes (25 μmol/L) in membranes containing these transporters, and other targets may be explored in future studies.

Although cabazitaxel is more active in MDR models, we previously reported that long-term drug selection with cabazitaxel alone resulted in *ABCB1* activation in a human breast cancer variant, MCF-7/CTAX [5]. We screened this variant for other ABC transporters but did not detect *ABCC1, ABCC2, ABCG2*, or *ABCC10* transcripts by qPCR. The taxane resistance observed in MCF-7/CTAX was multifactorial with mechanisms of resistance also observed in non-MDR variants resulting from counter selection with P-gp inhibitors. Following modulation with PSC-833, 3-fold residual resistance to cabazitaxel remained in MCF-7/CTAX that was associated with elevated class III β-tubulin (TUBB3), alterations in cell cycle regulators, and the induction of EMT [5].

We found that cabazitaxel's greater activity in *ABCB1*(+) models was due to its lower affinity for P-gp compared to the first-generation taxanes, docetaxel and paclitaxel. However, substantial cross-resistance to cabazitaxel was observed in the MDR models tested.

Author contributions Conception and design: GED, DS, DAG, SM, BIS. Development of methodology: GED, BIS. Acquisition of data (provided animals, acquired and managed patients, provided facilities, etc.): GED, VD, DW, NP, JB, JA. Analysis and interpretation of data (e.g., statistical analysis, biostatistics, computational analysis): GED, VD, DW, NP, JB, JA, DS, DAG, SM, BIS. Writing, review, and/or revision of the manuscript: GED, DAG, SM, BIS. Administrative, technical, or material support (i.e., reporting or organizing data, constructing databases): GED, DAG. Study supervision: GED, DAG, BIS. Other (chemical synthesis of radiolabeled taxanes and azido-taxanes): VD, DW, NP, JB, JA. Other (providing background information to help on study conception): DAG.

Funding G. E. Duran and B. I. Sikic received Grant support from Sanofi and from the U.S. National Institutes of Health (NIH) through the National Cancer Institute (R01 CA114037 and R01 CA184968).

Compliance with ethical standards

Conflict of interest The Stanford authors received grant support from Sanofi, while Drs. Derdau, Weitz, Philippe, Blankenstein, Atzrodt, Sémiond, Gianolio, and Macé are employees of Sanofi. They have no other potential financial conflicts of interest.

Ethical approval This article does not contain any studies with human participants or animals performed by any of the authors.

References

1. Giannakakou P, Sackett DL, Kang Y-K, Zhan Z, Buters JT, Fojo T et al (1997) Paclitaxel-resistant human ovarian cancer cells have mutant beta-tubulins that exhibit impaired paclitaxel-driven polymerization. J Biol Chem 272:17118–17125
2. Kajiyama H, Shibata K, Terauchi M, Yamashita M, Ino K, Nawa A et al (2007) Chemoresistance to paclitaxel induces epithelial-mesenchymal transition and enhances metastatic potential for epithelial ovarian carcinoma cells. Int J Cancer 31(2):277–283
3. Işeri OD, Kars MD, Arpaci F, Atalay C, Pak I, Gündüz U (2011) Drug resistant MCF-7 cells exhibit epithelial-mesenchymal transition gene expression pattern. Biomed Pharmacother 65(1):40–45
4. Yang Q, Huang J, Wu Q, Cai Y, Zhu L, Lu X et al (2014) Acquisition of epithelial–mesenchymal transition is associated with Skp2 expression in paclitaxel-resistant breast cancer cells. Br J Cancer 110:1958–1967
5. Duran GE, Wang YC, Francisco EB, Rose JC, Martinez FJ, Coller J et al (2015) Mechanisms of resistance to cabazitaxel. Mol Cancer Ther 14(1):193–201
6. Chabalier C, Lamare C, Racca C, Privat M, Valette A, Larminat F (2006) BRCA1 downregulation leads to premature inactivation of spndle checkpoint and confers paclitaxel resistance. Cell Cycle 5(9):1001–1007
7. Lafarge S, Sylvain V, Ferrara M, Bignon YJ (2001) Inhibition of BRCA1 leads to increased chemoresistance to microtubule-interfering agents, an effect that involves the JNK pathway. Oncogene 20(45):6597–6606
8. Mullan PB, Quinn PE, Gilmore PM, McWilliams S, Andrews H, Gervin C et al (2001) BRCA1 and GADD45 mediated G2/M cell cycle arrest in response to antimicrotubule agents. Oncogene 20:6123–6131
9. Quinn JE, James CR, Stewart GE, Mulligan JM, White P, Chang GKF et al (2007) BRCA1 mRNA expression levels predict for overall survival in ovarian cancer after chemotherapy. Clin Cancer Res 13(24):7413–7420
10. Quinn JE, Kennedy RD, Mullan PB, Gilmore PM, Carty M, Johnston PG et al (2003) BRCA1 functions as a differential modulator of chemotherapy-induced apoptosis. Can Res 63:6221–6228
11. Sung M, Giannakakou P (2013) BRCA1 regulates microtubule dynamics and taxane-induced apoptotic cell signaling. Oncogene 33(11):1418–1428
12. Srivastava RK, Mi QS, Hardwick JM, Longo DL (1999) Deletion of the loop region of Bcl-2 completely blocks paclitaxel-induced apoptosis. Proc Natl Acad Sci USA 96(7):3775–3780
13. Tang C, Willingham MC, Reed JC, Miyashita T, Ray S, Ponnathpur V et al (1994) High levels of p26 BCL2 oncoprotein retard taxol-induced apoptosis in human pre-B leukemia cells. Leukemia 8:1960–1969
14. Reed JC (1999) Bcl-2 family proteins: relative importance as determinants of chemoresistance in cancer. In: Hickman JA, Dive C (eds) Apoptosis and Cancer Chemotherapy, Humana Press, Totowa, NJ
15. Wang YC, Juric D, Francisco B, Yu RX, Duran GE, Chen GK et al (2006) Regional activation of chromosomal arm 7q with and without gene amplification in taxane-selected human ovarian cancer cell lines. Genes Chromosomes Cancer 45(4):365–374
16. Horwitz S, Cohen D, Rao S, Ringel I, Shen H, Yang C (1993) Taxol: mechanisms of action and resistance. J Natl Cancer Inst 15:55–61
17. Dumontet C, Duran GE, Steger KA, Beketic-Oreskovic L, Sikic BI (1996) Resistance mechanisms in human sarcoma mutants derived by single-step exposure to paclitaxel (Taxol). Cancer Res 56:1091–1097
18. Boyerinas B, Park SM, Murmann AE, Gwin K, Montag AG, Zillardt MR et al (2012) Let-7 modulates acquired resistance of ovarian cancer to Taxanes via IMP-1-mediated stabilization of MDR1. Int J Cancer 130(8):1787–1797
19. Vrignaud P, Sémiond D, Lejeune P, Bouchard H, Calvet L, Combeau C et al (2013) Preclinical antitumor activity of cabazitaxel, a semisynthetic taxane active in taxane-resistant tumors. Clin Cancer Res 19(11):2973–2983
20. Sémiond D, Sidhu SS, Bissery MC, Vrignaud P (2013) Can taxanes provide benefit in patients with CNS tumors and in pediatric patients with tumors? An update on the preclinical development of cabazitaxel. Cancer Cheother Pharmacol 72(3):515–528
21. Duran GE, Ford JM, Sikic BI (2000) A paclitaxel-resistant mutant with altered p53-dependent MAP4 expression and drug binding. In: Proceedings of the 91st annual meeting of the American Association for Cancer Research; 1–5 April 2000; San Francisco, CA. AACR, Philadelphia
22. Lacayo NJ, Duran GE, Sikic BI (2003) Modulation of resistance to idarubicin by the cyclosporin PSC 833 (valspodar) in multidrug-resistant cells. J Exp Ther Oncol 3:127–135
23. de Ravel M, Alameh G, Melikian M, Mahiout Z, Emptoz-Bonneton A, Matera E-L et al (2015) Synthesis of new steroidal inhibitors of P-glycoprotein-mediated multidrug resistance and biological evaluation on K562/R7 erythroleukemia cells. J Med Chem 58:1832–1845
24. Ginot L, Jeammesson P, Angiboust J-F, Jardillier J-C, Manfait M (1984) Interactions of adriamycin in sensitive and resistant leukemic cells: a comparative study by microspectrofluorometry. Stud Biophys 104:145–153
25. Spicakova T, O'Brien MM, Duran GE, Sweet-Cordero A, Sikic BI (2010) Expression and silencing of the microtubule-associated protein Tau in breast cancer cells. Mol Cancer Ther 9(11):2970–2981
26. Minotti AM, Barlow SB, Cabral F (1991) Resistance to antimitotic drugs in chinese hamster ovary cells correlates with changes in the level of polymerized tubulin. J Biol Chem 266:3987–3994
27. Chen CKLN., Duran GE, Cohen D, Sikic BI (2000) Loss of cyclosporin and azidopine binding are associated with altered ATPase activity by a mutant P-glycoprotein with deleted Phe335. Mol Pharm 57:769–777
28. Orr GA, Rao S, Swindell CS, Kingston DG, Horwitz SB (1998) Photoaffinity labeling approach to map the Taxol-binding site on the microtubule. Methods Enzymol 298:238–252
29. Rao S, Orr GA, Chaundhary AG, Kingston DG, Horwtiz SB (1995) Characterization of the taxol binding site on the microtubule. 2-(*m*-Azidobenzoyl)taxol photolabels a peptide (amino acids 217–231) of beta-tubulin. J Biol Chem 270(35):20235–20238
30. Wu Q, Bounaud PY, Kuduk SD, Yang CP, Ojima I, Horwtiz SB et al (1998) Identification of the domains of photoincorporation of the 3′- and 7-benzophenone analogues of taxol in the carboxyl-terminal half of murine mdr1b P-glycoprotein. Biochemistry 37(32):11272–11279
31. Ojima I, Geney R, Ungureanu IM, Li D (2002) Medicinal chemistry and chemical biology of new generation taxane antitumor agents. IUBMB Life 53(4–5):269–274
32. Fletcher J, Haber M, Henderson M, Norris M (2010) ABC transporters in cancer: more than just drug efflux pumps. Nat Rev Cancer 10:147–156